J. Phycol. **38,** 1024–1039 (2002)

PHYLOGENETIC POSITION OF *CRUSTOMASTIX STIGMATICA* SP. NOV. AND *DOLICHOMASTIX TENUILEPIS* IN RELATION TO THE MAMIELLALES (PRASINOPHYCEAE, CHLOROPHYTA)[1]

Adriana Zingone,[2] *Marco Borra, Christophe Brunet, Gandi Forlani, Wiebe H. C. F. Kooistra, and Gabriele Procaccini*

Stazione Zoologica "Anton Dohrn", Villa Comunale, 80121 Naples, Italy

A new marine microalga from the Mediterranean Sea, *Crustomastix stigmatica* Zingone, is investigated by means of LM, SEM, TEM, and pigment and molecular analyses (nuclear-encoded small subunit [SSU] rDNA and plastid-encoded *rbc*L). Pigment and molecular information is also provided for the related species *Dolichomastix tenuilepis* Throndsen et Zingone. *Crustomastix stigmatica* has a bean-shaped cell body 3–5 μm long and 1.5–2.8 μm wide, with two flagella four to five times the body length. The single chloroplast is pale yellow-green, cup-shaped, and lacks a pyrenoid. A small bright yellow stigma is located in the mid-dorsal part of the cell under the chloroplast membrane. An additional accumulation of osmiophilic globules is at times seen in a chloroplast lobe. Cells lack flat scales, whereas three different types of hair-like scales are present on the flagella. The main pigments of C. *stigmatica* are those typical of Mamiellales, though siphonein/siphonaxanthin replaces prasinoxanthin and uriolide is absent. The pigment pool of *D. tenuilepis* is more similar to that of *Micromonas pusilla* (Butcher) Manton et Parke and of other Mamiellales. The nuclear SSU rDNA phylogeny shows that the inclusion of *C. stigmatica* and *D. tenuilepis* in the Mamiellales retains monophyly for the order. The two species form a distinct clade, which is sister to a clade including all the other Mamiellales. Results of *rbc*L analyses failed to provide phylogenetic information at both the order and species level. No unique morphological or pigment characteristics circumscribe the mamiellalean clade as a whole nor its two daughter clades.

Key index words: Crustomastix stigmatica; *Dolichomastix tenuilepis*; **Mamiellales; Mediterranean Sea; phylogeny; pigments; Prasinophyceae; *rbc*L; SSU rDNA; taxonomy; ultrastructure**

Abbreviations: **MgDVP, Mg-2,4-divinyl pheoporphyrin a_5 momomethyl ester; ML, maximum likelihood; MP, maximum parsimony; NJ, neighbor joining; *rbc*L, large subunit of the RUBISCO encoding gene**

Prasinophyceae are a paraphyletic assemblage of unicellular algae containing chl *a* and *b*. The fact that they have been considered the ancestors of all green algae and embryophyte land plants (i.e. the Viridiplantae *sensu* Cavalier-Smith [1981]) has placed them in the spotlight of phylogenetic research (Melkonian 1990, Sym and Pienaar 1993, Steinkötter et al. 1994, Daugbjerg et al. 1995, Nakayama et al. 1998, Fawley et al. 2000). Currently Prasinophyceae include about 20 genera of flagellated and coccoid marine microalgae, some of which have been described only in recent years. EM studies have revealed considerable morphological and ultrastructural heterogeneity. The presence of a flagellar pit, parabasal bodies (Golgi), and muciferous bodies was initially considered as distinctive characteristics but was then shown to be neither unique nor universal for Prasinophyceae (Sym and Pienaar 1993). Several sets of variously shaped scales on the cell and flagellar surface have been described and used for taxonomy and identification. The internal architecture, the configuration of the flagellar apparatus, and other specific cell organelles are other morphological characters on which phylogenetic relationships have been inferred (Sym and Pienaar 1993). Pigment composition has also been used to support phylogenetic relationships, highlighting a notable diversity among species despite a rather homogeneous plastid structure (Sym and Pienaar 1993, Egeland et al. 1995a,b).

Molecular analyses based on the large subunit of the RUBISCO encoding gene (*rbc*L) (Daugbjerg et al. 1995) and on the nuclear small subunit (SSU) rDNA (Nakayama et al. 1998, Fawley et al. 2000) have revealed that prasinophyceans are paraphyletic, thus confirming their morphological and biochemical heterogeneity. At least five major prasinophycean lineages exist within the Chlorophyta (Nakayama et al. 1998, Fawley et al. 2000). The relationships among these lineages and other clades with green algae and higher plants are not fully resolved as yet nor have distinctive morphological and biochemical features been identified for each prasinophycean lineage. Molecular results have also shown that scale-less coccoid species appear in several distinct lineages, demonstrating frequent and independent events of reduction in characters across the Prasinophyceae (Courties et al. 1998, Fawley et al. 2000).

The order Mamiellales constitutes one of the major prasinophycean lineages. Five genera were confirmed

[1] Received 11 March 2002. Accepted 3 June 2002.

[2] Author for correspondence: e-mail zingone@alpha.szn.it.

to belong to this order based on molecular data: *Mamiella*, *Mantoniella*, *Micromonas* (SSU and *rbc*L data; Daugbjerg et al. 1995, Nakayama et al. 1998, Fawley et al. 2000), *Bathycoccus* (*rbc*L data; Daugbjerg et al. 1995), and *Ostreococcus* (SSU data; Courties et al. 1998). For two other genera, *Dolichomastix* and *Crustomastix*, only morphological features are known (Manton 1977, Moestrup 1990, Throndsen and Zingone 1997, Nakayama et al. 2000). Based only on morphological information, the phylogenetic position of these genera is difficult to infer. Indeed, some *Dolichomastix* species possess scales that differ from those of other Mamiellales, whereas *Crustomastix didyma* Nakayama, Kawachi et Inouye, the only species known for this genus, has a specialized cell covering but lacks body and flagellar scales and a pyrenoid (Nakayama et al. 2000). Lack of features could be interpreted as a primitive condition, yet in the Mamiellales it has been demonstrated to result from secondary losses (Daugbjerg et al. 1995, Nakayama et al. 1998).

Here we describe a new flagellate species, *Crustomastix stigmatica* Zingone sp. nov., based on morphological, pigment, and molecular data (nuclear-encoded SSU rDNA and plastid-encoded *rbc*L). We also provide information on pigments, nuclear SSU rDNA, and *rbc*L of *Dolichomastix tenuilepis* Throndsen et Zingone and discuss the phylogenetic position of the two genera, *Crustomastix* and *Dolichomastix*, in relation to the Mamiellales.

MATERIALS AND METHODS

Cultures. A unialgal culture of *C. stigmatica*, pras1, was established by serial dilution of a seawater sample collected with a Niskin bottle in the Gulf of Naples (station MC, 40° 49′ N, 14 °15′ E), Mediterranean Sea on 14 May 1995. The authentic strain of *D. tenuilepis*, Caprim2-4II, was obtained from serial dilution cultures of a seawater samples collected with Niskin bottles at a station south of the Island of Capri (14°16′E, 40° 30′N), Mediterranean Sea on 6 July 1994. The strain of *Micromonas pusilla*, MP1, used for pigment analysis, was isolated from the station MC on 8 April 1993. The three cultures were maintained in K medium (Keller et al. 1987) without the addition of silicates, adjusted at a salinity of 36 psu. Cultures were kept at 20–24° C and a 12:12-h light:dark cycle at 100 μmol photons·m^{-2}·s^{-1} emitted from cool-white fluorescent tubes.

LM observations were made on exponentially growing cultures with a Zeiss Axiophot microscope (Carl Zeiss, Oberkochen, Germany) equipped with Nomarski differential interferential contrast, phase contrast, and bright-field optics. Light micrographs were taken using a Zeiss Axiocam digital camera.

EM preparations. For TEM ultrathin sections, culture material of *C. stigmatica* was fixed in glutaraldehyde 1% or 2% followed by osmium tetroxide as described in Zingone et al. (1995). Additional preparations were made using buffered glutaraldehyde 2.5% with and without the addition of a few drops of osmium tetroxide, followed by osmium tetroxide, as indicated in Nakayama et al. (2000). For whole-mount observations, a drop of culture was placed on a TEM grid and fixed with osmium tetroxide vapors (Moestrup and Thomsen 1980) or with glutaraldehyde 2.5% or 1.25% (Marin and Melkonian 1994). Grids were rinsed with distilled water, dried, and then stained with 0.5% uranyl acetate. Whole mounts and ultrathin sections were observed using a Philips 400 transmission electron microscope (Philips Electron optics BV, Eindhoven, The Netherlands). Specimens prepared for SEM were fixed with osmium tetroxide, treated as indicated in Zingone et al. (1995), and observed using a Philips 505 SEM.

Morphological information provided for *C. stigmatica* is based on approximately 250 EM micrographs. In the description, the cell orientation proposed by Christensen (1980) is followed, with the flagellar insertion defining the ventral side of the cell and the foremost part during swimming considered as anterior. When cells are observed from the dorsal side, with their anterior part at the top, the cell's right side is on the observer's right. This orientation also allows the distinction of the right and the left flagellum. The numbering of the basal bodies and root terminology correspond to those indicated in Moestrup (2000).

Pigment analysis. Between 5 and 10 mL of cultures of *C. stigmatica*, *D. tenuilepis*, and *M. pusilla* in exponential growth phase were filtered through GF/F filters (25 mm, Whatman Ltd., Maidstone, UK) that were frozen at −80° C until analysis. Frozen filters were extracted in 4 mL of absolute methanol by mechanical grinding, and the extracts were filtered through Whatman GF/F filters. The three strains were analyzed twice on two different HPLC systems, using two different methods, Laboratoire Interdisciplinaire des Sciences de l'Environnement (LISE) and Stazione Zoologica di Napoli (SZN), to obtain a more effective separation of carotenoids in case of coelution of different pigments. Identification and quantification of single pigments were realized using chl and carotenoid standards obtained from the VKI (Water Quality Institute) International Agency for ^{14}C Determination, Denmark. Unfortunately, some pigments (unknown pigments) were not quantified. In the LISE method, the culture extract was injected in a Beckman System Gold HPLC (Beckman Coulter, Fullerton, CA, USA), following the procedure of Vidussi et al. (1996). A 3-μm C_8 BDS column (100 × 4.6 mm, Thermo Hypersil-Keystone, Runcorn, UK) was used, and the mobile phase was composed of two solvent mixtures: A, methanol:aqueous ammonium acetate (70:30) and B, methanol. The gradient between the solvents was the same as in Vidussi et al. (1996). Absorbance was detected at 440 nm using a model 168 Beckman photodiode array detector to obtain the 400–600 nm spectrum for each pigment. Fluorescence was measured using an Sfm 25 Kontron spectrofluorometer (Kontron Instruments, Watford, UK) with excitation at 407 nm and emission at 660 nm. For the SZN method, the culture extract was injected in a Hewlett Packard series 1100 HPLC (Hewlett-Packard, Wilmington, NC, USA). The column was a C_{18} ODS Ultrasphere Beckman (150 × 4.6 mm). The two solvent mixtures were as follows: A, methanol:aqueous ammonium acetate (80:10:10) and B, methanol:ethyl acetate (70:30). The solvent flux was 1.5 mL·min^{-1}, and the analysis duration was 20 min. Pigments were detected at 440 nm using a Hewlett Packard photodiode array detector model DAD series 1100, which gives the 400- to 700-nm spectrum for each detected pigment. Names and abbreviations used for pigments follow the SCOR nomenclature (Jeffrey et al. 1997).

DNA extraction, PCR, and sequencing. For molecular analysis, cultures of *C. stigmatica* and *D. tenuilepis* were harvested during the exponential growth phase by centrifugation. Total nucleic acid extractions were performed using a modified 2× hexadecyltrimethylammonium bromide procedure (Doyle and Doyle 1990). Total nucleic acid preparations were used as template for the amplification of the nuclear SSU rDNA and *rbc*L genes. PCR amplifications were performed in a Hybaid PCR Express machine (Thermo Hybaid, Ashford, UK) using the primers ss5 and ss3 (Rowan and Powers 1992) for nuclear SSU rDNA (30 cycles of 1 min at 94° C, 1 min at 52° C, and 2 min at 72° C) or the primers RH1S and CE1161R (Daugbjerg et al. 1994) for *rbc*L (30 cycles of 1 min at 94° C, 1 min at 55° C, and 2 min at 72° C) and Taq DNA polymerase (Boehringer, Mannheim, Germany). Additional primers were designed for PCR amplifications of the internal regions of both genes (Table 1). Amplified DNA fragments were purified with the QIAEX II purification kit (Qiagen Genomics, Bothell, WA, USA) and directly sequenced on a Beckman Ceq 2000 automatic sequencer, using Dye-Terminator cycle sequencing kit (Beckman). Resulting sequence phenograms were analyzed using the software package DNASTAR (DNASTAR, Madison, WI, USA).

Phylogenetic analysis. Genes from different compartments of the cell (i.e. the nuclear-encoded SSU rDNA and the plastid-encoded *rbc*L) were selected to obtain independent hypotheses of the phylogenetic relationships between *C. stigmatica* and *D. tenuilepis*. Sequences used for comparison were chosen across

TABLE 1. Primer sequences used to amplify and sequence the nuclear SSU rDNA and *rbc*L in *Crustomastix stigmatica* and *Dolichomastix tenuilepis*.

Primer code	Direction[a]	Sequence (5′-3′)	Position
Nuclear SSU rDNA			
Common			
ss5[b]	F	GGTTGATCCTGCCAGTACTCATATGCTTG	
ss3[b]	R	GATCCTTCCGAGGTTCACCTACGGAAACC	
Rev	R	ATGGTAGGCCTCTATCCTACCATCGA	291 (*D. tenuilepis*) 298 (*C. stigmatica*)
Specific for *C. stigmatica*			
PraD1	F	CTACCACATCCAAAGGAAAGGCAG	384
PraD3	F	GCATGGAATAACACTATAGGACCT	784
PraR1	R	CCAGAACATCTAAGGGCATCACAG	1485
PraR4	R	TCCGTCAATTCCCTTTAAGTTTCA	1180
Specific for *D. tenuilepis*			
D1	F	ACGAAGGGACGTGTTTATTAGA	102
D2	F	AAATCCCTTAACGAGGATCCATTG	496
D4	F	CATTGTCAGAGGTGAAATTCTTGG	863
D5	R	TTTGATTTCTCATAAGGTGCTGAC	1040
D3	R	CACATTGTCCCTCTAAGAAGTCAG	1328
*rbc*L			
Common			
RH1S[c]	F	ATGTCACCACAAACAGAAACT	
CE1161R[c]	R	CATGTGCAATACGTCAATACC	
Specific for *C. stigmatica*			
PRH1S2	F	CTGTTACGTTTCATACCCACTTG	255
PCE1161R2	R	TACAACAGTTCCTGAGTGTAGG	936
PDW3	R	GCACGGTGAATGTGAAGAAG	829
Specific for *D. tenuilepis*			
DRH1S2	F	GCATACGTAGCATACCCACTTG	259
DCE1161R2	R	GCTGCACGCTTCATCATTTCATC	706

[a]F, forward; R, reverse.
[b]PCR primers, designed by Rowan and Powers (1992).
[c]PCR primers, designed by Daugbjerg et al. (1994).

the chl *a*+*b* algae (Tables 2 and 3). As outgroups for sequence comparison we selected *Cyanophora paradoxa* (Glaucocystophyceae) for the *rbc*L and the latter species and *Chlorarachnion reptans* (Chlorarachniophyceae) for the SSU rDNA. Merged sequences were aligned by eyeball in Se-Al v1.d1 (Rambaud 1995). The *rbc*L sequences aligned without problems; only those positions were removed that would otherwise disrupt first, second, and third codon positional arrangement. Two regions in the nuclear SSU rDNA sequence (i.e. the tip of the V4 region and the loop at the tip of the terminal stem region in the secondary structure) revealed ambiguous multiple alignment possibilities and were therefore removed. The final alignment comprised approximately 1700 base pairs per sequence over 1774 positions.

Phylogenetic significance of informative sites was assessed by comparing the measure of skewedness (g_1 value) obtained under the random trees option in PAUP* (version 4.0b8; Swofford 2001) with empirical threshold values in Hillis and Huelsenbeck (1992). Substitution model and parameters describing among site-rate variation were estimated using Modeltest 3.0 (Posada and Crandall 1998) and then imported into neighbor joining (NJ) and maximum likelihood (ML) analyses in PAUP*. Weighted maximum parsimony (MP) phylogenies were inferred using the heuristic search procedure with the tree bisection/reconnection, branch swapping algorithm, and the Goloboff fit criterion (K = 2) option in PAUP*. Bootstrap values for clades were obtained with 1000 replicates for NJ and MP (without weighting). Extra base changes needed to explain alternative topologies were evaluated using MacClade (Maddison and Maddison 1992). This program was also used to translate *rbc*L DNA sequences into amino acid sequences.

RESULTS

Crustomastix stigmatica Zingone sp. nov.

Cellula phaseoliformis, 3–5 μm longa et 1.5–2.8 μm lata, concava cum superficie ex qua duo flagella pauci dissimili longitudine oriuntur cum cellulae superficie acutissimum angulum facerent. Chloroplastus unus, lobis duobus, sine pyrenoide. Stigma quod singula lamella constitutum est, sub chloroplasti membrana ab opposita parte flagellorum principii, collocatum est. Cellulae sine squamis. Breves pili (longitudine 0.3 μm circiter) a flagellorum lateribus dispositi sunt; pili terminales (longitudine 0.5 μm circiter) terni dispositi sunt et 40 sub-unitates comprehendunt; pauci et longi pili (1.9 μm circiter) in parte basali unius ex flagellis sunt et 36–38 sub-unitates comprehendunt.

Cells bean-shaped, 3–5 μm long, 1.5–2.8 μm wide. Flagella inserted in the concave side of the cell, with a very acute angle to the cell surface. One chloroplast with two lobes and without a pyrenoid. Stigma consisting of a single layer in a parietal position in the mid-dorsal part of the cell, opposite to the flagellar insertion. Cells lacking flat scales. Flagellar T-hair scales about 0.3 μm long. Tip hair scales in bundles of three, about 0.5 μm long, composed of 40 subunits. A few P_l-hairs, about 1.9 μm long located along the proximal part of one flagellum, with 36–38 globular subunits.

Holotype: Embedding Pras1/N6OS deposited at the Stazione Zoologica "Anton Dohrn", Naples, Italy.

Type locality: Gulf of Naples

Etymology: The specific epithet refers to the presence of an eyespot, or stigma.

LM and SEM. Cells are bean-shaped (Figs. 1, A–E, and 2, A and B), usually about 3–4 μm long and 2 μm wide. The two flagella range from 10.4 to19.2 μm and are subequal in size, the right flagellum or flagellum 2

TABLE 2. GenBank accession numbers for sequenced taxa used in nuclear SSU rDNA phylogenetic analysis.

Organism	Accession no.
Acrosiphonia duriuscula (Ruprecht) Yendo	AB049418
Chara foetida Braun	X70704
Chlorarachnion reptans Geitler	X70809
Chlorarachnion CCMP242	U03479
Coccoid green alga CCMP1205	U40921
Coccoid green alga CCMP1220	U40920
Coccoid green alga CCMP1407	U40919
Coccoid prasinophyte CCMP1193	AF203399
Coccoid prasinophyte CCMP1413	AF203402
Coleochaete scutata Brébisson	X68825
Crustomastix stigmatica Zingone	AF509628
Cyanophora paradoxa Korshikoff	X68483
Cymbomonas tetramitiformis Schiller	AB017126
Doliochomastix tenuilepis Throndsen et Zingone	AF509625
Dunaliella salina (Dunal) Teodoresco	M84320
Genicularia spirotaenia (Ramb.) de Bary	X74753
Halosphaera sp. Shizugawa	AB017125
Hydrodictyon reticulatum (L.) Lagerheim	M74497
Mamiella sp.	AB017129
Mantoniella antarctica Marchant	AB017128
Mantoniella squamata (Manton et Parke) Desikachary	X73999
Marchantia polymorpha L.	X75521
Mesostigma viride Lauterbom	AJ250109
Micromonas pusilla (Butcher) Manton et Parke	AJ010408
Nephroselmis olivacea Stein	X74754
Nephroselmis pyriformis CCMP717[a]	X75565
Ostreoccocus tauri Courties et Chrétiennot-Dinet	Y15814
Prasinococcus sp. CCMP1194	AF203400
Prasinophyte symbiont of radiolarian	AF166381
Pseudoscourfieldia marina (Throndsen) Manton	AF122888
Pterosperma cristatum Schiller	AB01727
Pycnococcus provasolii Guillard	X91264
Pycnococcus provasolii Guillard CCMP1198[b]	AJ010406
Pyramimonas disomata Butcher	AB017121
Pyramimonas olivacea N. Carter	AB017122
Pyramimonas parkeae Norris et Pearson	AB017124
Pyramimonas propulsa Moestrup et Hill	AB017123
Scenedesmus pupukensis (Kalina et Punčochářová) Kessler et al.	X91267
Scherffelia dubia (Perty) Pascher	X68484
Staurastrum sp.	X77452
Tetraselmis striata Butcher	X70802
Trebouxia impressa Ahmadjian	Z21551
Ulothrix zonata (Weber et Mohr) Kütz	Z47999
Zamia pumila L.	M20017

[a]Listed in GenBank as *Pseudoscourfieldia marina*.
[b]Listed in GenBank as "unidentified prasinophyte."

TABLE 3. GenBank accession numbers for sequenced taxa used in *rbc*L phylogenetic analysis.

Organism	Accession no.
Bathycoccus prasinos Eikrem et Throndsen	U30275
Bryopsis plumosa (Hudson) C. Agardh	AB038480
Caulerpa racemosa (Forsskål) J. Agardh	AB038486
Codium lucasii Setchell	AB038481
Coleochaete orbicularis Pringsheim	L13477
Crustomastix stigmatica Zingone	AF509626
Cyanophora paradoxa Korshikoff	X53045
Cymbomonas tetramitiformis Schiller	L34687
Dolichomastix tenuilepis Throndsen et Zingone	AF509627
Genicularia spirotaenia (Ramb.) de Bary	U71439
Halimeda discoidea Decaisne	AB038488
Halimeda opuntia (L.) J.V. Lamouroux	AB038489
Mamiella sp.	U30277
Mantoniella squamata (Manton et Parke) Desikachary	U30278
Marchantia polymorpha L.	U87079
Mesostigma viride Lauterbom	U30282
Micromonas pusilla (Butcher) Manton et Parke	U30276
Nephroselmis minuta (N. Carter) Butcher	U30286
Nephroselmis olivacea Stein	U30285
Pedinomonas sp. PCC441	U30287
Pseudoscourfieldia marina (Throndsen) Manton	U30279
Pterosperma cristatum Schiller	U30281
Pycnococcus provasolii Guillard	U30280
Pyramimonas cirolanae Pennick	L34776
Pyramimonas cyclotreta Daugbjerg	L34814
Pyramimonas cyrtoptera Daugbjerg	L34819
Pyramimonas grossii Parke	L34779
Pyramimonas mantoniae Moestrup et Hill	L34810
Pyramimonas mitra Moestrup et Hill	L34812
Pyramimonas moestrupii McFadden	L34811
Pyramimonas octopus Moestrup et Aa. Kristiansen	L34817
Pyramimonas olivacea N. Carter	L34815
Pyramimonas orientalis MacFadden	L34813
Pyramimonas parkeae Norris et Pearson	L34816
Pyramimonas propulsa Moestrup et Hill	L34777
Pyramimonas sp.	L34834
Pyramimonas sp. "greenland"	L34818
Pyramimonas tetrarhyncus Schmarda	L34833
Pyramimonas tychotreta Daugbjerg	L34778
Resultor mikron (Throndsen) Moestrup	U30288
Staurastrum pingue Teiling	AF203506
Tetraselmis aff. *maculata* Butcher	U30283
Tetraselmis marina (Cienk.) Norris, Hori et Chihara	U30284
Trebouxia anticipata (Ahmadjian in Ed.) Archibald	AF189069
Zamia furfuracea L. fil.	AF202959

(F2) being slightly shorter than the left one (F1) (Figs. 1C and 2A). They emerge laterally from a slight depression in the concave side of the cell (Fig. 2B). They have pointed ends (Fig. 2A) and are directed almost always backward (Figs. 1, B–E, and 2, A and B). The chloroplast is pale yellow-green, with two lobes. A distinct bright-yellow stigma lies in a parietal position in the dorsal part of the cell, opposite to the flagellar insertion (Fig. 1, A, B, and D). An additional eyespot is seen at times in the posterior part of the cell (Fig. 1D). At SEM no scales are seen. The cell surface is smooth, especially in the area corresponding to the chloroplast lobes. Dividing cells are found with each old flagellum paired with a short new flagellum (Fig. 2C).

Cells move along circular paths, returning more or less in the same position regularly. Some cells appear to rotate around their anterior pole (Fig. 1E). Flagella are kept backward, each forming a wide S-shaped figure, with the two "S" mirror imaged to each other (Fig. 1E). Slower cells are seen to rotate around the anteroposterior axis while moving, whereas faster cells seem to glide around this axis. It is difficult, however, to establish whether this gliding is real or an optical effect caused by rotation. When cells stop, the flagella are shed quickly and dissolve in a few seconds, leaving only a pale trace.

TEM. TEM whole mounts (Fig. 3, A–F) confirm the absence of body and flagellar scales other than three types of hair scales. A few P_I-hairs (*sensu* Marin and Melkonian 1994), 1.9 μm long, are found along the proximal part of the shorter flagellum (Fig. 3A). These hair scales comprise a proximal shaft (Fig. 3, B and C), 1.2 μm long, a distal part consisting of 36–38

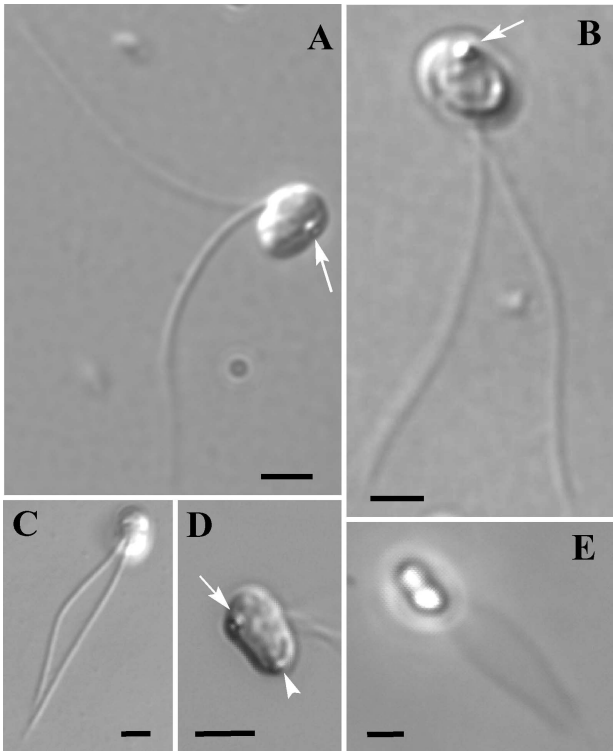

FIG. 1. Light microscope images of *Crustomastix stigmatica*. (A–D) Nomarski differential interferential contrast. (E) Phase contrast. Scale bar, 2 μm. (A) Lateral outline of a cell, with a dorsal eyespot (arrow). (B) Cell with two subequal flagella and a dorsal eyespot (arrow). (C) Cell in ventral view, showing the insertion point of the flagella. (D) Cell with a dorsal eyespot (arrow) and an additional eyespot (arrowhead) in the posterior end. (E) Living cell rotating around the anterior pole, with the two flagella directed backward, forming a wide S-shaped figure.

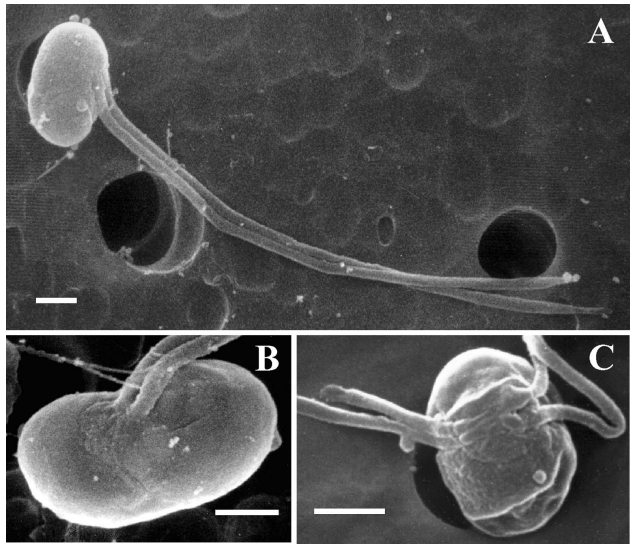

FIG. 2. SEM of *Crustomastix stigmatica*. Scale bar, 1 μm. (A) Whole cell with the two flagella, the right one shorter than the left one. (B) Cell in lateral-ventral view, showing the bean-shaped body and the flagellar insertion. (C) A division stages, showing a very short new flagellum to the left.

globular subunits, and a faint terminal filament 0.5 μm long. Tip hair scales, 0. 5 μm long, are present at the pointed ends of both flagella in bundles of three (Fig. 3, D and E). They comprise one larger basal subunit and about 50 globular subunits and bear a distal filament 0.7 μm long (Fig. 3E). Lateral T-hair scales (Fig. 3F) are about 0.4 μm long, tubular in shape, and bear a short (0.1 μm) faint filament at both ends.

In ultrathin sections (Figs. 4, A–L, and 5, A–E), a round-oval nucleus with a large nucleolus occupies a large part of the chloroplast-free cell space in the right side of the cell (Fig. 4, A, C–E, and F). To the left, a long sausage-shaped mitochondrion (Fig. 4G), circular to oval in cross-section (Fig. 4, A–C, and E), runs more or less adjacent to the inner chloroplast face along the anteroposterior axis of the cell, slightly obliquely. A well-developed Golgi apparatus is present ventrally with respect to the mitochondrion, in the left side of the cell close to the flagellar bases (Fig. 4, B and C). An inconspicuous microbody is at times detected adjacent to the ventral side of the chloroplast (Fig. 4B). Vesicles with granular or particulate material abound (Fig. 4, B and E). A membrane similar to the external cell envelope surrounds these structures. Some vesicles contain a fibrous material (Fig. 4I). A single chloroplast is located in a parietal position along the dorsal and lateral sides of the cell (Fig. 4, A–F), expanding into two lobes (Fig. 4, A and F) at the anterior and posterior poles. The chloroplast is surrounded by a double membrane and consists of three to five lamellae, each formed by three thylakoids, immersed in a granular matrix (Fig. 4H). A pyrenoid is absent, and one or two starch accumulations are seen in some sections (Fig. 4D). An eyespot or stigma formed by a single layer of osmiophilic globules is located in the dorsal part of the chloroplast, opposite to the flagellar insertion (Fig. 4, A–C). Up to nine globules are counted in a single tangential section (Fig. 4K). A similar aggregate of osmiophilic globules is visible at times in one of the chloroplast lobes (Fig. 4J). Cell body and flagella appear to be covered by a double-layer membrane, with the external layer not markedly thicker than the internal one (Fig. 4L).

The basal bodies (Fig. 5, A–E) are about 700 nm long. They form an acute angle with the ventral surface of the cell (Figs. 4A and 5, A and B) and among themselves (Fig. 5E). A distal fiber connects the basal bodies (Fig. 5, C–E). Two microtubular roots emerge from basal body 1 (Fig. 5, C and D). The 1d root, corresponding to R1 in the root terminology proposed by Moestrup (2000), consists of three microtubules (Fig. 5, C and D) and runs under the cell membrane toward the posterior pole of the cell (Fig. 5A). The 1s (= R2) root shows a 3+1 microtubular pattern in its proximal part (Fig. 5D). Neither a multilayered structure nor a rhizoplast were observed.

Pigments. The two methods used gave comparable results. Absorbance chromatograms (440 nm) obtained

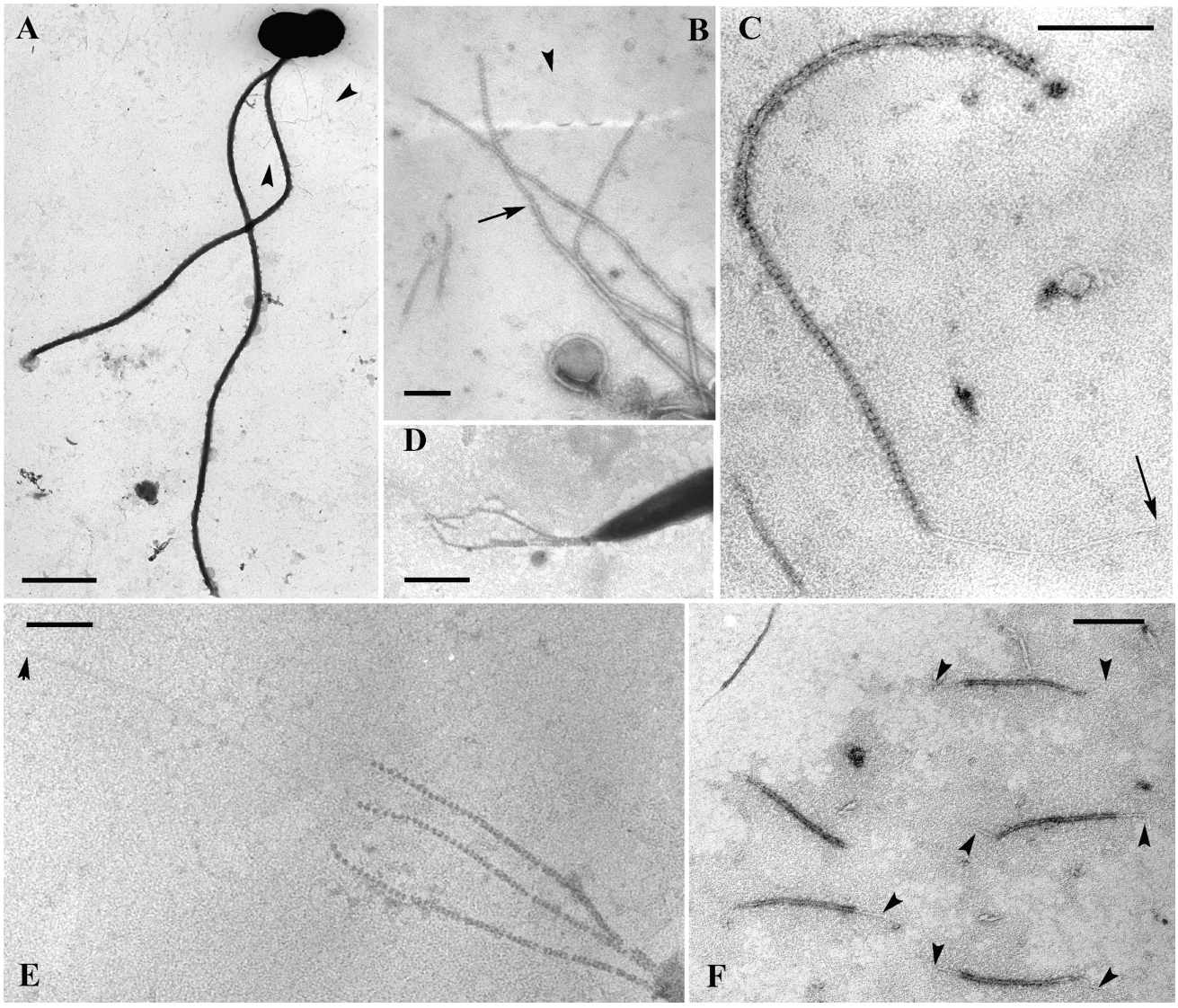

FIG. 3. TEM of whole mounts of *Crustomastix stigmatica*. Scale bars: A, 2 μm; B–D and F, 0.2 μm; E, 1 μm. (A) Whole cell with long flagella; arrowheads point at P_1 flagellar hair scales. (B) Three P_1 flagellar hair scales; arrow points to the transition between the proximal shaft and the globular subunits. (C) P_1 flagellar hair scale; the arrowhead indicates the tip of the distal filament. (D) Tip hairs at the end of the pointed flagellar end. (E) A group of three tip hairs with long distal filaments (arrowhead). (F) Lateral T hairs. Note faint filaments at both ends (arrowheads).

with the LISE method are presented in Figure 6, and their related peaks are listed in Table 4. To compare the pigment content among the three species analyzed (*C. stigmatica*, *D. tenuilepis*, and *M. pusilla*) and with other existing data, ratios of the different quantified accessory pigments on chl *a* are presented in Table 5. More than 20 pigments, 8 of which form the major peaks, were detected (Fig. 6, Tables 4 and 6).

Molecular phylogeny. The nuclear SSU rDNA: Length distribution of 10,000 random trees was highly skewed, indicating significant phylogenetic signal in the SSU rDNA alignment ($g_1 = -1.6545$ given 425 parsimony informative sites). Results from Modeltest indicated high sequence complexity and nonrandom distribution of changes across the SSU rDNA. The phylogeny resulting from ML analysis constrained with optimal Modeltest parameters revealed a series of well-supported lineages (Fig. 7). Our results indicate paraphyletic Prasinophyceae. Topology among the lineages remained poorly resolved and changed considerably depending on outgroup choice. Even with all outgroups removed from the analysis, the topology among the lineages remained poorly resolved (Fig. 7). Nonetheless, outgroup choice did not affect the topology within the lineages.

Dolichomastix tenuilepis and *C. stigmatica* were recovered as sister species. Together they formed a well-supported sister clade to an equally well-supported clade with the remainder of the Mamiellales. Altogether, these taxa are recovered in one of the principal prasinophycean lineages. A tree resulting from weighted MP

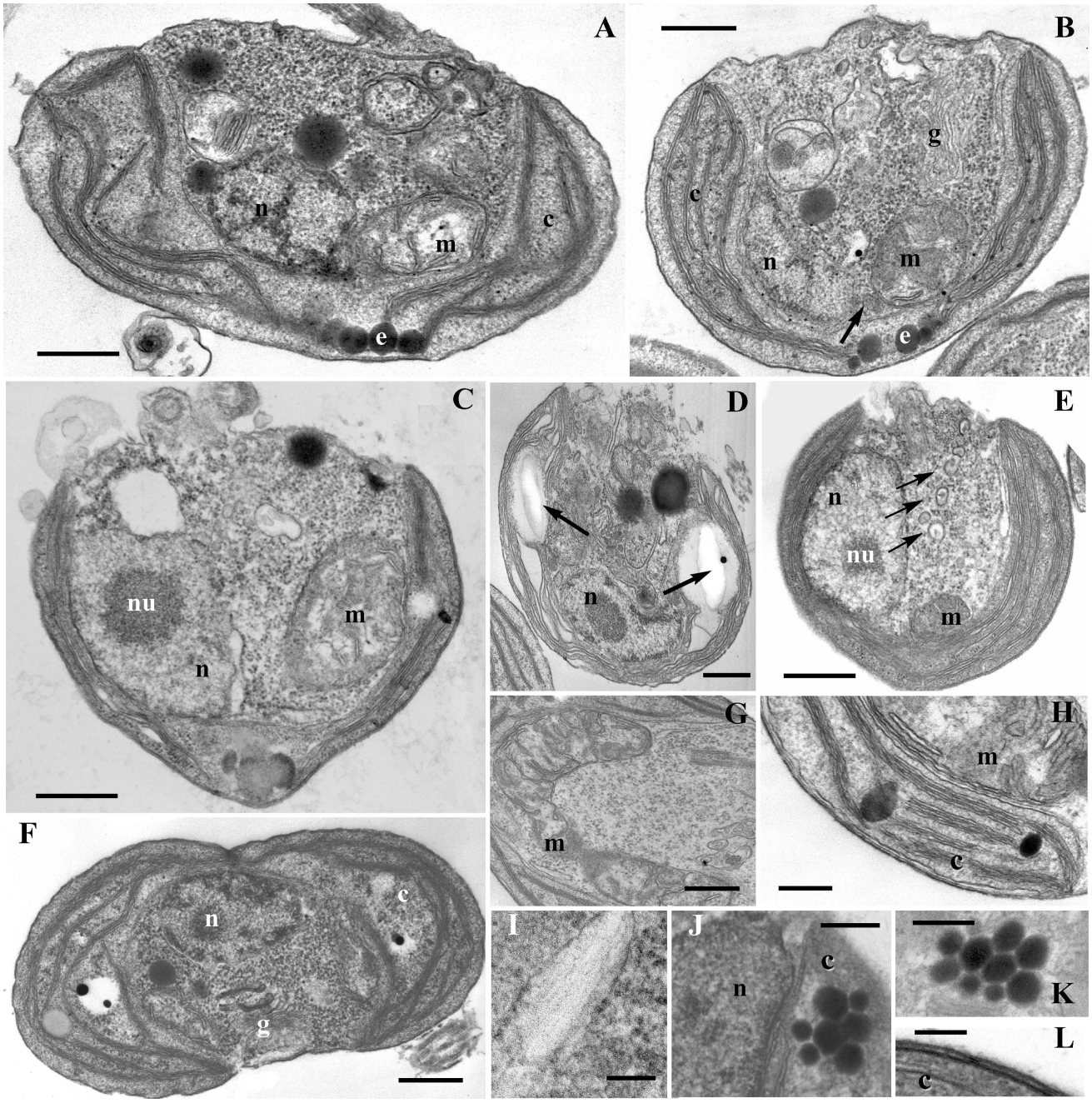

FIG. 4. Ultrastructural features of *Crustomastix stigmatica*, TEM. Scale bars: A–G, 0.5 μm; H–K, 0.2 μm; J and L, 0.1 μm. (A) Longitudinal section through the insertion of flagellum 1. (B) Transversal section showing a well-developed Golgi body. (C) Transversal section at the level of the flagellar insertion. (D) Transverse section showing starch granules (arrows) in both chloroplast lobes. (E) Transverse section showing an array of circular inclusions (arrows). (F) Longitudinal section perpendicular to the one showed in A. (G) Oblique section through the mitochondrion. (H) Ultrastructural detail of the chloroplast, with four lamellae. (I) A vesicle with fibrillar material. (J) Tangential section of an eyespot in a chloroplast lobe. (K) Tangential section of an eyespot with nine osmiophilic globules. (L) Section through the cell envelope, close to the chloroplast, showing the double layer of electron-dense material. c, chloroplast; g, Golgi body; m, mitochondrion; n, nucleus; nu, nucleolus.

analysis (K = 2, tree not shown) revealed the same topology for the Mamiellales. Results of bootstrap analysis showed high support for this topology, yet topology among the principal lineages of the green algae remains poorly resolved. Choice of radically different values for K in weighted MP analyses resulted in different topologies among the principal lineages but did not affect topology within Mamiellales.

The rbc*L:* Initial K2P distance analysis of only third positions in the *rbc*L alignment revealed massive satu-

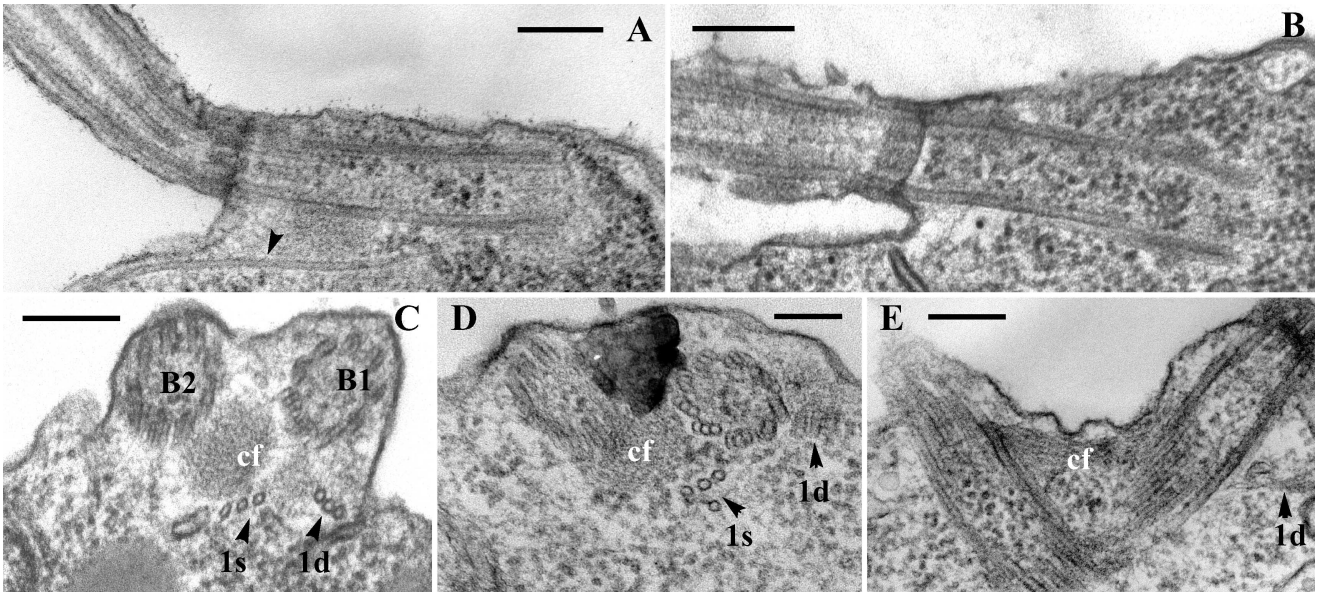

FIG. 5. Ultrastructural features of flagellar bases of *Crustomastix stigmatica*, TEM. Scale bar, 0.2 μm. (A) Basal body of flagellum 1, with root 1d running backward under the cell surface (arrowhead). (B) Basal body of flagellum 2. (C) Transverse section across the flagellar bases showing roots 1s, 1d, and the connecting fiber. (D) Proximal transverse section across the flagellar bases. (E) Tangential section of the flagellar bases. cf, connecting fiber; 1s, 1d, right and left microtubular flagellar roots.

ration, with distances among taxa ranging between 0.3 and 1.5. Even within *Pyramimonas* species, distances between 0.11 and 0.55 were observed. High substitution saturation was also inferred from a virtually normal distribution of tree lengths among 10,000 randomly generated trees. If only first and second codon positions were included, obtained K2P distances within the ingroups ranged between 0.02 and 0.15, yet bootstrap support for most clades was low. In an attempt to improve resolution within and among ingroups, we removed the outgroup taxon. Nevertheless, basal ramifications among clades obtained insufficient boot-

TABLE 4. Pigment distribution in the three species analyzed.

Peak no.	Retention time	*M. pusilla*	*D. tenuilepis*	*C. stigmatica*	Pigment
1	4.01	+	+	+	MgDVP
2	5.84	+	Traces	−	Uriolide
3	6.30	−	−	+	Siphonaxanthin
4	6.80	+	+	−	Prasinoxanthin
5	7.01	+	+	+	Violaxanthin
6	7.35	+	−	Traces	Unk. a[a]
7	7.67	+	−	−	Unk. b[a]
8	8.09	+	+	+	Neoxanthin
9	8.17	+	−	−	Antheraxanthin
10	8.36	+	−	−	Unk. c
11	8.63	+	−	−	Unk. d
12	9.50	−	+	+	Lutein
13	9.58	−	−	+	Zeaxanthin
14	10.02	+	−	−	Unk. e
15	11.88	+	+	+	Unk. f
16	12.25	+	+	+	Chl *b* allom
17	12.51	+	+	+	Chl *b*
18	12.80	+	+	+	Chl *b*′
19	14.20	−	+	−	Chl *a* allom
20	14.40	+	+	+	Chl *a* allom
21	14.70	+	+	+	Chl *a*
22	15.04	+	−	+	Chl *a*′
23	15.40	−	+	+	Unk. g
24	15.67	+	−	−	Unk. h
25	16.17	+	−	−	Unid. M1-like[a]
26	17.32	−	−	+	α-Carotene
27	17.38	+	+	+	β-Carotene

[a]Pigments considered in Table 6 for comparison.

TABLE 5. Pigment ratios (μg/μg) in the three species analyzed.

Pigment ratios	*M. pusilla*	*D. tenuilepis*	*C. stigmatica*
Chl			
MgDVP/chl *a*	0.28	0.22	0.11
Chl b/chl *a*	0.24	0.46	0.37
MgDVP/total chl	0.18	0.13	0.08
Chl *b*/total chl	0.16	0.27	0.25
Chl *a*/total chl	0.66	0.59	0.67
Carotenoids			
Siphonaxanthin/chl *a*	0	0	0.12
Prasinoxanthin/chl *a*	0.61	0.22	0
Violaxanthin/chl *a*	0.25	0.65	0.20
β-Carotene/chl *a*	0.009	0.013	0.038
Lutein/chl *a*	0.001	0.021	0.003

strap support. If only *D. tenuilepis*, *C. stigmatica*, and the Mamiellales were included as ingroups and *Nephroselmis* spp. as outgroup, the data set did not contain sufficient phylogenetic signal (insignificant g_1 value). The same is true for larger groupings with only prasinophyceans and *Tetraselmis* as outgroup and with only 1 and 2 positions included. However, if all positions were included, the bootstrap values basically showed *D. tenuilepis* and *C. stigmatica* collapsing in a basal polytomy. An NJ tree inferred from the alignment of amino acid residues of the *rbc*L sequences (tree not shown) at least grouped Mamiellales with *D. tenuilepis* and *C. stigmatica* in a clade, although with only 51% bootstrap support and lacking any internal structure. Results of MP bootstrap analysis also provided only marginal support (53%) for such a grouping. Therefore, basically *rbc*L failed to provide phylogenetic information at the taxonomic level of relationships across mamiellalean genera.

DISCUSSION

Morphology and taxonomy of Crustomastix stigmatica. The flagellate described here is attributed to the monospecific genus *Crustomastix* based on the morphological similarity with its type species, *C. didyma*, recently described from the northwestern Pacific (Nakayama et al. 2000). The two species share a number of features, which include the bean-like cell shape, lateral insertion of the flagella, general arrangement of the body organelles, and absence of a pyrenoid. Both species lack flat scales and have similar flagellar hair scales. T-hair scales only are different in *C. didyma*, having one row of distal globular subunits in addition to the proximal tubular shaft. The thin crust forming the cell covering, which gives the name to the genus (crusta = crust, mastix = a whip, flagellum), is a character less prominent and difficult to detect. Similarly to *M. pusilla* (Manton 1959), *C. stigmatica* possesses a membrane consisting of two distinct electron dense layers, but differently from *C. didyma*, the outermost layer is not significantly thicker than the inner one. In LM, cells lose their shape as soon as they stop moving, whereas flagella dissolve in a few seconds once they are shed. These observations confirm the extremely fragile nature of the external cell and flagellar envelope, which probably explains the irregularities seen in EM sections at the cell surface. In *C. didyma*, a "crust" is only revealed with specific fixation procedures (Nakayama et al. 2000), and therefore the cell envelope could be as delicate as in *C. stigmatica*. Unless the crust is an artifact of the fixation procedure, it is also possible that it can be revealed in other scale-bearing or naked prasinophyceans as well, provided that the appropriate fixation procedures are applied.

The main character distinguishing *C. stigmatica* from *C. didyma* (Table 7) is the consistent presence of a conspicuous stigma in the central part of the chloro-

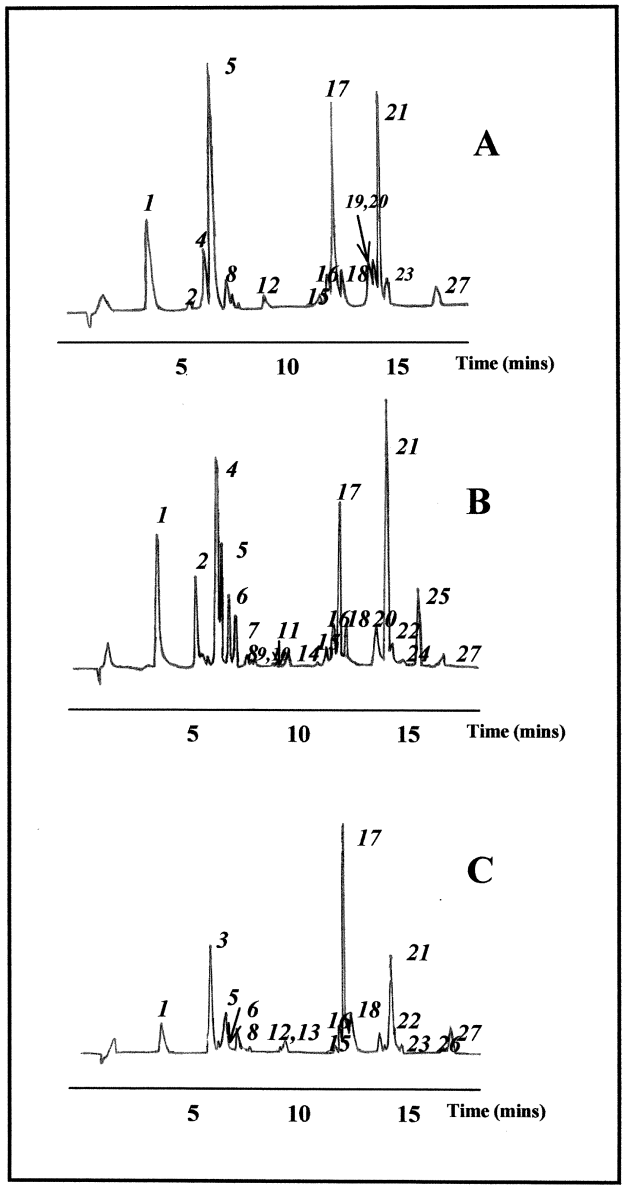

FIG. 6. HPLC absorbance (440 nm) chromatogram of (A) *Dolichomastix tenuilepis*, (B) *Micromonas pusilla*, and (C) *Crustomastix stigmatica* obtained with the LISE method (Vidussi et al. 1996). For peak identification, see Table 4.

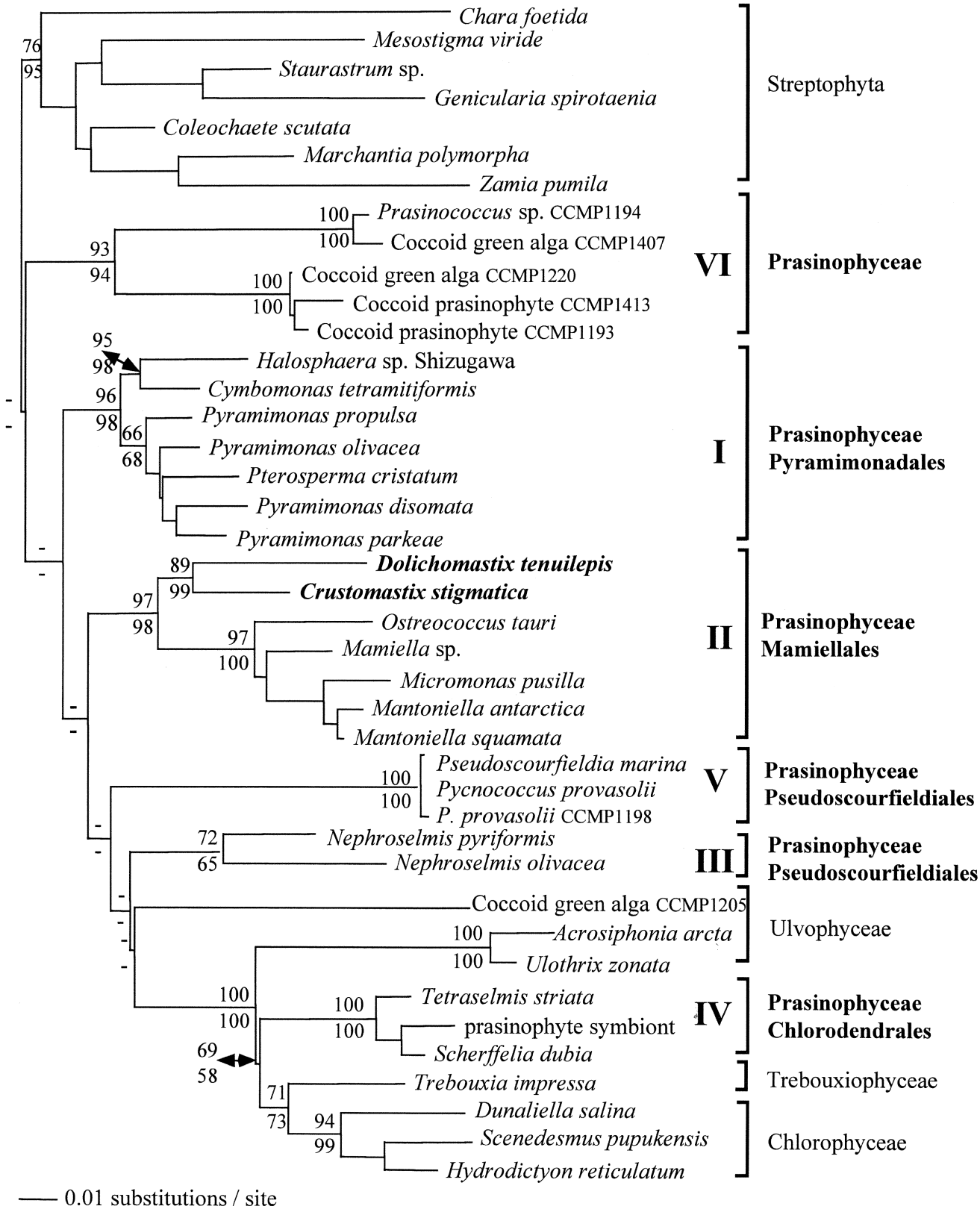

FIG. 7. ML phylogram inferred from nuclear SSU rDNA sequences of 41 taxa (see Table 2). Proportion of sites assumed to be invariable = 0.4689; rates assumed to follow a gamma distribution with shape parameter = 0.6224. Assumed substitution rates: A⇔G = 2.447, C⇔T = 4.784, all other substitution rates are 1.000 by default (Modeltest: TrN + I + G); −Ln likelihood = 12328.739; length = 1266, consistency index = 0.467, retention index = 0.600. Values above internodes of major clades indicate MP bootstrap values (1000 replicates, full heuristic search with TBR branch swapping option); those below internodes are bootstrap values (1000 replicates NJ trees of ML distances under the same Modeltest parameter settings). A "-" indicates a bootstrap value less than 50%. Bootstrap values associated with minor clades have been omitted for clarity. Streptophyta have been positioned as outgroup. Prasinophycean clade numbering follows Fawley et al. (2000).

TABLE 6. Comparison of absorption characteristics of three unidentified carotenoids.

Pgiment	Reference	Species	Absorption (nm)
Unid. M1-like	This study	*Micromonas pusilla*	(420), 443, 471
M1	Fawley 1992	*Mantoniella squamata*	(420), 443, 470
Pigment 11	Wilhelm et al. 1997	*M. squamata*	445–474
Unk. a	This study	*Crustomastix stigmatica*, *M. pusilla*	(406), 427, 453
Unknown 1	Fawley 1992	*M. pusilla*	(405), 427, 453
Micromonol	Wilhelm et al. 1997	*M. squamata*	428.1 and 454.6
Micromonol	Egeland et al. 1995b	*M. pusilla*, *M. squamata*	427 and 452
Unk. b	This study	*M. pusilla*	458
Micromonal	Wilhelm et al. 1997	*M. squamata*	459.5
Micromonal	Egeland et al. 1995a	*Bathycoccus prasinos*	450 (in acetone)
Micromonal	Egeland et al. 1995b	*M. pusilla*, *M. squamata*, *Pseudoscourfieldia marina*	450 (in acetone)

plasts. This is visible in LM as a bright-yellow refringent body and in TEM as a group of electron-dense vesicles tightly apressed. Some lipid vesicles are described in the same position in *C. didyma*; however, they are smaller and not seen in LM. In addition, a second eyespot in a chloroplast lobe, which is frequently seen in *C. stigmatica*, is not described for *C. didyma*. The presence of additional pigmented granules in the chloroplast has previously been used as distinctive character, for example, in *Pyramimonas plurioculata* Butcher (Butcher 1959).

Crustomastix didyma differs from *C. stigmatica* also in the presence of a duct, a deep invagination of the plasmalemma opening in the ventral surface of the cell. This structure was revealed in *C. didyma* only by a special fixation procedure (Nakayama et al. 2000), like the cell coat. We repeated the same procedure three times and observed 100 ultrathin TEM sections without finding any convincing evidence of the presence of a duct in *C. stigmatica*. Though it seems unlikely, we cannot exclude the possibility that a duct was not observed due to unnoticed differences in the fixation procedure or in culture conditions.

In the flagellar apparatus, a multilayered structure associated with root 1d is described for *C. didyma* (Nakayama et al. 2000). This structure was not detected in *C. stigmatica*. Other peculiar characteristics of *C. stigmatica* are the absence of a rhizoplast and the extremely small size and scarce visibility of the microbody. The latter was ambiguously identified only based on its presumed position. These differences again could reflect fixation problems; however, both a rhizoplast and a microbody were clearly discernible in ultrathin sections of *D. tenuilepis* prepared for TEM in the same laboratory with the same procedure as that used for *C. stigmatica* (Throndsen and Zingone 1997).

Despite the resemblance in shape, most cells of *C. stigmatica* are consistently shorter than the minimum length indicated for *C. didyma* (i.e. 4 μm) in both living and glutaraldehyde-fixed material. The width of *C. stigmatica* fell more frequently within the range indicated for C. *didyma* (2–3 μm). Differences were also noticed in the swimming behavior. However, these observations need verification using the same conditions of vessels and light.

In conclusion, differences and affinities between *C. didyma* and *C. stigmatica* support the erection of a new species and its attribution to *Crustomastix*, respectively. Yet the taxonomic importance of characters in Mamiellales is not fully known; therefore, molecular information on *C. didyma* will be valuable to confirm the relationships between the two species.

Pigment composition. The pigment suites of *C. stigmatica* and *D. tenuilepis* reflect the high diversity and heterogeneity found in the pigment pool of the class Prasinophyceae (Sym and Pienaar 1993, Egeland et al. 1995a,b, 1997, Wilhelm et al. 1997). The two species share with *M. pusilla* chl *a* and *b* and Mg-2,4-divinyl pheoporphyrin a_5 momomethyl ester (MgDVP). Ratios of chl *a* over total chl in the three species are similar to the values reported for another mamiellalean alga, *Bathycoccus prasinos* (Egeland et al. 1995b). The chl *b*/chl *a* ratios are lower than values reported in many studies (Hooks et al. 1988, Fawley 1992, Simon et al. 1994, Chrétiennot-Dinet et al. 1995, Jeffrey and Vesk 1997) but similar to those found by Egeland et al. (1995a).

Large differences exist in the carotenoid content among *C. stigmatica*, *D. tenuilepis*, and *M. pusilla*. *Crustomastix stigmatica* lacks prasinoxanthin and uriolide but possesses siphonaxanthin. A similar pigment suite has been found in other prasinophyceans, including the mamiellalean *Ostreococcus tauri* (Chrétiennot-Dinet et al. 1995). The pigment suite of *D. tenuilepis* is instead more similar to that of *M. pusilla* and of the rest of known Mamiellales. However, the relative content of prasinoxanthin is much lower in *D. tenuilepis* than

TABLE 7. Main morphological characteristics separating *Crustomastix didyma* and *C. stigmatica*.

Species	Size (μm)	Eyespot	Duct	Multilayered structure	Rhizoplast	Microbody	Flagellar T hairs
C. didyma	2–3 × 4–6	Small lipid globules, not visible in LM	Present	Present	Present	Clearly detected	With globular subunits
C. stigmatica	1.5–2.8 × 3–5	Clearly visible in LM	Undetected	Undetected	Undetected	Inconspicuous	Without globular subunits

in *M. pusilla*. A comparably wide range of prasinoxanthin/chl *a* ratios has been found in prasinoxanthin-containing Prasinophyceae (Fawley 1992, Simon et al. 1994). Hooks et al. (1988) separated them into two groups, with a discriminating threshold ratio of 0.2. Following this classification, *D. tenuilepis* would correspond to the limit between the two groups, whereas *M. pusilla* belongs to the second group (ratio > 0.2). Thus, the three species examined encompass the whole range of variability for prasinoxanthin content, including its absence.

The pigment uriolide also shows considerable differences among the three species examined. It is absent in *C. stigmatica* but produces a high surface peak in *M. pusilla*. Its presence in *D. tenuilepis* is not fully confirmed, because only traces of a pigment with the same retention time as uriolide were found. Other differences are the higher values of β-carotene/chl *a* ratio in *C. stigmatica* and the absence of α-carotene in *M. pusilla* and *D. tenuilepis*. Some of the unidentified carotenoids found in our analyses, that is, the unidentified M1-like "unknown a" and "unknown b" pigments, have similar absorption properties and probably correspond to unidentified pigments found in *M. pusilla*, *M. squamata*, and other prasinophyceans by other authors (Table 6).

Another peculiar feature in pigment composition of *C. stigmatica* is the presence of high amounts of zeaxanthin. In green algae, zeaxanthin is involved in the photodependent xanthophyll interconversion cycle and is synthesized from violaxanthin under light stress (Demming-Adams 1990). In *C. stigmatica*, zeaxanthin could be synthesized under lower light intensity than in *M. pusilla* and *D. tenuilepis*, which lacked zeaxanthin. *Dolichomastix tenuilepis* showed a rather high violaxanthin/chl *a* ratio as compared with *C. stigmatica* and *M. pusilla*. Violaxanthin is the principal carotenoid in some prasinophyceans, including *Ostreococcus tauri* (Chrétiennot-Dinet et al. 1995) and *Pyramimonas parkeae* (Kohata and Watanabe 1989) and the Mesostigmatophyceae *Mesostigma viride* (Fawley and Lee 1990). However, differences in pigment ratios could also be related to growth conditions, especially light quantity (Fawley 1992), day length, and diel variations (Kohata and Watanabe 1989), as well as to ecophysiological characteristics of the clones examined (Guillard et al. 1991).

Differences in pigment compositions in closely related species are difficult to explain, because functional implications of presence/absence and replacements of pigments are not fully clarified. High proportion of chl *b* could be an adaptation for growth at low light (Yokohama 1981). The presence of MgDVP, with maximum of absorption at 439 nm (i.e. between the absorption maxima of chl *a* and chl *b*) could further increase the capacity of light absorption in the blue region of the spectrum, thus suggesting an adaptation to an ecological niche deep in the water column. The xanthophylls siphonein and siphonaxanthin also absorb light in the blue-green and green part of the spectrum (500–550 nm) (Yokohama 1981, Anderson 1983) and efficiently transfer light excitation energy to chl *a* (Anderson 1983). They could correspond to an adaptation of algae to deep green coastal waters (Yokohama 1981, 1983). Prasinoxanthin and siphonaxanthin seem to be functionally comparable (Wilhelm et al. 1986), although the absorption maximum of prasinoxanthin (457 nm) is narrower than that of siphonaxanthin (446–466 nm). Notably, many prasinophyceans have been isolated from deep layer (Guillard et al. 1991, Simon et al. 1994), so an efficient light-harvesting and excitation transfer systems to chl *a* could be an adaptation of these algae to a low light environment.

Phylogeny of C. stigmatica *and* D. tenuilepis. The phylogeny inferred from nuclear SSU rDNA shows that *C. stigmatica* and *D. tenuilepis* are distantly related sister species within Mamiellales. To confirm both their inclusion and their basal position in this order, we had to add representatives of all other chl *a*+*b* orders to the phylogenetic survey. The nuclear SSU rDNA phylogeny failed to resolve relationships among these orders unambiguously but adequately resolved relationships within them, confirming results obtained with similar data by other authors (Courties et al. 1998, Nakayama et al. 1998, Fawley et al. 2000). Based on morphological characters of *C. didyma*, Nakayama et al. (2000) suggested that the genus *Crustomastix* represents an early divergence from other Mamiellales and a "missing link" between the Mamiellales and the Pyramimonadales. Although nuclear SSU rDNA analysis confirms the basal position of *Crustomastix* within the Mamiellales, low bootstrap values do not allow to resolve properly the phylogenetic relationships of this genus with other orders of the prasinophyceans.

Results of our *rbc*L analysis did not resolve phylogenetic relationships at the levels needed for this study; they even failed to assess the phylogenetic position of species within single clades. These results are similar to those shown by Daugbjerg et al. (1995), who obtained little or no bootstrap support for major prasinophycean clades.

Recovery of *C. stigmatica* and *D. tenuilepis* as nearest neighbors in a sister clade to the remainder of the Mamiellales allows erection of a monophyletic sister order to monophyletic Mamiellales *sensu stricto*. Yet their inclusion in the Mamiellales also retains monophyly for the order. The questions that we have to deal with next is whether a single clade with Mamiellales can be circumscribed with shared derived character states and whether the two sister clades can be delimited likewise.

Phylogenetic status of morphological features in Mamiellales. The addition of *C. stigmatica* and *D. tenuilepis* retains monophyly for the Mamiellales but does not help identify any unifying and distinctive morphological character for the order (Table 8). The order Mamiellales was erected for scale-bearing Prasinophyceae lacking a proximal layer of square- or diamond-shaped scales (Moestrup 1984). Initially, the order only in-

cluded the flagellate genera *Mantoniella*, *Mamiella*, *Dolichomastix*, and the coccoid *Bathycoccus* (Moestrup 1990). Most species in these genera possess body and flagellar scales with a spider-web pattern formed by concentric and radiating ribs. Only two of the four *Dolichomastix* (i.e. *D. nummulifera* and *D. tenuilepis*) have scales without radiating ribs. Subsequently, phylogenies inferred from *rbc*L (Daugbjerg et al. 1995) and SSU rDNA (Nakayama et al. 1998) demonstrated that the scale-less uniflagellate *M. pusilla* also belongs to Mamiellales. Both phylogenies demonstrated that absence of scales and presence of a single very short flagellum in *M. pusilla* result from secondary loss because the species appears in an advanced position in the Mamiellales. Lack of traits is even more pronounced in *Ostreococcus tauri*, the smallest eukaryotic organism known at present (Courties et al. 1994). This species not only lacks scales but also flagella and a pyrenoid (Chrétiennot-Dinet et al. 1995). Our SSU phylogeny confirms results of Courties et al. (1998) that this tiny coccoid species belongs to the Mamiellales.

The genus *Dolichomastix* was erected to include species with very long flagella (Manton 1977), a feature thereafter shown not to be diagnostic for the genus (Throndsen and Zingone 1997). It was included in the Mamiellales due to the lack of underlayer scales (Moestrup 1984, 1990, Moestrup and Throndsen 1988). The position of the flagellar insertion and the general architecture of body organelles of *D. tenuilepis* (Throndsen and Zingone 1997), very similar to those of *Mamiella* and *Mantoniella* species, further supported this inclusion. As for the genus *Crustomastix*, Nakayama et al. (2000) tentatively attributed the scale-less species *C. didyma* to the Mamiellales based on the combination of several microanatomical features, including organelle configuration, position and structure of transitional region of the flagella, and absence of a microtubular root associated with the second basal bodies. However, as these authors pointed out, single states associated to these characters in the Mamiellales are probably homoplasies, because they also exist in species belonging to other prasinophycean orders. Indeed, no single morphological feature can be identified that is unique to the Mamiellales nor that is present in all the species of the order.

Our results also confirm nonmonophyly for the two families of the Mamiellales, namely, the Mamiellaceae and Micromonadaceae, which group scale-bearing and scale-less Mamiellales, respectively. In fact, the phylogenetic position of *M. pusilla* and *Ostreococcus tauri* clearly showed that the two families are nonmonophyletic (Fawley et al. 2000). Similarly to the main clade of the Mamiellales, the clade formed by *D. tenuilepis* and *C. stigmatica* is not homogeneous, the former species having body and flagellar scales with concentric ribs, the latter lacking scales. Therefore, the families Mamiellaceae and Micromonadaceae have representatives in both clades of the Mamiellales. This is not surprising, because the absence of scales, and in general morphological reduction or missing characters, have occurred as a result of secondary loss all across prasinophycean clades and therefore cannot reliably define phylogenetic groups. Another example is provided, in the order Pseudoscourfieldiales, by the scale-bearing flagellate *Pseudoscourfieldia marina* and the scale-less coccoid *Pycnococcus provasolii*. These two species show a high genetic similarity (Daugbjerg et al. 1995, Fawley et al. 1999), which suggests that they represent different stages of the life cycle of two closely related species.

The only morphological character that could circumscribe the clade formed by *D. tenuilepis* and *C. stigmatica* as distinct from the main mamiellalean clade is the shape of flagellar T hairs. Species of the genus *Mantoniella* and *Mamiella* have two rows of globular subunits on the flagellar T hairs, which according to Nakayama et al. (1998) would be a truly shared derived state of the order. In *D. tenuilepis* and *C. stigmatica*, T hairs consist instead only of a tubular shaft with thin and short filaments at one or both ends, respectively. However, the state of this character in other species attributed to the genera *Dolichomastix* and *Crustomastix* is not homogeneous. In *C. didyma*, flagellar T hairs have one row of subunits in addition to the

TABLE 8. Morphological features and pigments of species attributed to the order Mamiellales.

Species	Flagella	Spider-web scales	Circular patterned scales	Pyrenoid	MgDVP	Prasinox.	Siphonax.	Uriolide	T hairs: tubular shaft	T hairs: globular subunits
Bathycoccus prasinos	−	+	−	−	+	+	−	+		
Crustomastix didyma	2	−	−	−	?	?	?	?	+	+
Crustomastix stigmatica	2	−	−	−	+	−	+	−	+	−
Dolichomastix eurylepidea	2	+	−	?	?	?	?	?	?	?
Dolichomastix lepidota	2	+	−	?	?	?	?	?	−	+
Dolichomastix nummulifera	2	−	+	?	?	?	?	?	?	?
Dolichomastix tenuilepis	2	−	+	+	+	+	−	?	+	−
Mamiella gilva	2	+	−	+	+	+	−	+	+	+
Mantoniella squamata	2	+	−	+	+	+	−	+	−	+
Mantoniella antarctica	2	+	−	+	+	+	−	+	−	+
Micromonas pusilla	1	−	−	+	+	+	−	+	−	−
Ostreococcus tauri	−	−	−	−	+	−	+	−		

Characters were selected based on their relevance to the phylogenetic discussion.

tubular shaft (Nakayama et al. 2000). In *Dolichomastix*, T hairs have only been described for *D. lepidota* Manton (Throndsen and Zingone 1997), which has the two rows of globular subunits like *Mamiella* and *Mantoniella* species. Also the spider-web scales covering the cell body and flagella in *D. lepidota* and in *D. eurylepidea* Manton are closer to those of *Mantoniella squamata* than to the ones with concentric pattern of *D. nummulifera* Manton and *D. tenuilepis*. This suggests that the genus *Dolichomastix* could in fact include more than one genus (Moestrup 1990) and that *D. lepidota* could belong to *Mantoniella* (Throndsen and Zingone 1997).

Phylogenetic status of pigments in the Mamiellales. Different classification systems of Prasinophyceae have been proposed based on pigment composition. In the system proposed by Egeland et al. (1997), three groups are recognized. *Dolichomastix tenuilepis* would belong to the group 3, which is characterized by the presence of prasinoxanthin and/or uriolide and hence also includes *M. pusilla*, whereas *C. stigmatica* would belong to the group 2, due to the presence of siphonaxanthin. A higher heterogeneity within Mamiellales is shown according to a classification based on six distinct pigment groups (Sym and Pienaar 1993). In this system, most Mamiellales including *M. pusilla* belong to group 6, which is characterized by the presence of prasinoxanthin, MgDVP, and uriolide, along with minor unknown pigments. *Crustomastix stigmatica*, together with *O. tauri*, fits instead in group 4, which presents some pigment characteristics of Ulvophyceae (siphonein/siphonaxanthin and absence of prasinoxanthin) and others of Prasinophyceae (MgDVP). Finally, *D. tenuilepis* probably belongs to group 5, differing from species of group 6 due to the lack of a clear peak of uriolide as well as of several unknown pigments.

Phylogenetic structure of the Mamiellales as shown by molecular data (Fawley et al. 2000, this study) does not correspond with patterns in pigment data. Not a single pigment defines Mamiellales, nor the two clades identified within the order. C*rustomastix stigmatica* have a pigment suite clearly different from that of *D. tenuilepis* but similar to that of the naked coccoid *O. tauri*, which belongs to the major clade of the Mamiellales. In addition, *C. stigmatica* and *O. tauri* lack uriolide, which was previously believed to be shared by all species in the order Mamiellales (Nakayama et al. 1998), though is present in other clades as well.

Many pigments appear to be ancestral features of species. For instance, MgDVP is a common feature in all Mamiellales so far analyzed for pigments (Fawley 1992, this study). However, MgDVP is not unique for this order, because it has been found in other prasinophyceans (Ricketts 1970, Hooks et al. 1988) and even in a cryptophyte (Schimek et al. 1994). Another example of a possibly ancestral pigment is siphonein/siphonaxanthin, which is found in the Mamiellales *C. stigmatica* and *O. tauri* and in several unrelated species of the group 4, scattered across Pyramimonadales, Pseudoscourfieldiales, and Chlorodendrales (Sym and Pienaar 1993). Siphonein/siphonaxanthin have been considered an evolutionary relict of some Chlorophytes (Anderson 1983). Their loss in *M. pusilla* and in the other Mamiellales of the pigment groups 5 and 6 (Sym and Pienaar 1993) would be a more derived character state. Apparently, secondary loss or substitution of pigments are easy to occur, as also demonstrated by a strain of *M. pusilla* (CS-170) from the Coral Sea, Australia, indistinguishable from other strains, which lacks MgDVP but has a chl c_3-like pigment (Jeffrey 1989).

The mismatch between phylogeny and pigment composition revealed by the Mamiellales, and in general by the Prasinophyceae, also has meaningful consequences for chemotaxonomy. Despite the importance of pigment suites in taxonomic identification of species, the use of single pigments as taxonomic markers of higher taxonomic groups within prasinophyceans is presently impossible.

In conclusion, the addition of two new taxa to the Mamiellales has shown a higher level of diversity than originally assumed for this order. Our study has also confirmed that the former circumscriptions of Mamiellales and of families within the order are weak. Indeed, no sound character redefines the order Mamiellales based on morphological or pigment features or to distinguish families within the order. We also confirmed the nonmonophyly of the Prasinophyceae. To obtain a classification of Prasinophyceae that is both natural and taxonomically meaningful, a multitude of orders is needed along the grade leading to Ulvophyceae, Chlorophyceae, and Trebouxiophyceae. This conclusion is not surprising if one takes into account that all the lineages considered are very ancient and have presumably undergone many morphological and biochemical changes in the course of their long evolutionary history.

We thank Gennaro Iamunno for TEM embeddings and ultrathin sections and Augusto Passarelli and Ciro Chiaese for HPLC analyses with the SZN method. Thanks are also due to Prof. Jahn Throndsen (University of Oslo, Norway) for reading and commenting on the manuscript.

Anderson, J. M. 1983. Chlorophyll-protein complexes of a *Codium* species, including a light-harvesting siphonaxanthin-chlorophyll *a*/*b* protein complex, an evolutionary relic of some Chlorophyta. *Biochim. Biophys. Acta* 724:370–80.

Butcher, R. W. 1959. An introductory account of the smaller algae of the British coastal waters. Part I. Introduction and Chlorophyceae. *Fish. Invest.* 4:1–74.

Cavalier-Smith, T. 1981. The origin and early evolution of the eukaryotic cell. *In* Carlile, M. J., Collins, J. F. & Moseley, B. E. B. [Eds.] *Molecular and Cellular Aspects of Microbial Evolution.* Cambridge University Press, Cambridge, pp. 33–84.

Chrétiennot-Dinet, M. J., Courties, C., Vaquer, A., Neveux, J., Claustre, H., Lautier, J. & Machado, M. C. 1995. A new marine picoeucaryote: *Ostreococcus tauri* gen. et sp. nov. (Chlorophyta, Prasinophyceae). *Phycologia* 34:285–92.

Christensen, T. 1980. *Algae: A Taxonomic Survey.* AiO Tryk, Odense, 216 pp.

Courties, C., Perasso, R., Chrétiennot-Dinet, M.-J., Gouy, M., Guillou, L. & Troussellier, M. 1998. Phylogenetic analysis and genome size of *Ostreococcus tauri* (Chlorophyta, Prasinophyceae). *J. Phycol.* 34:844–9.

Courties, C., Vaquer, A., Troussellier, M., Lautier, J., Chrétiennot-Dinet, M. J., Neveux, J., Machado, C. & Claustre, H. 1994. Smallest eukaryiotic organism. *Nature Lond.* 370:255.

Daugbjerg, N., Moestrup, Ø. & Arctander, P. 1994. Phylogeny of the genus *Pyramimonas* (Prasinophyceae, Chlorophyta) inferred from the *rbc*L gene. *J. Phycol.* 30:991–9.

Daugbjerg, N., Moestrup, Ø. & Arctander, P. 1995. Phylogeny of genera of Prasinophyceae and Pedinophyceae (Chlorophyta) deduced from molecular analysis of the *rbc*L gene. *Phycol. Res.* 43:203–13.

Demming-Adams, B. 1990. Carotenoids and photoprotection in plants: a role for the xanthophyll zeaxanthin. *Biochim. Biophys. Acta* 1020:1–24.

Doyle, J. J. & Doyle, J. L. 1990. Isolation of plant DNA from fresh tissue. *Focus* 12:13–5.

Egeland, E. S., Eikrem, W., Throndsen, J., Wilhelm, C., Zapata, M. & Liaaen-Jensen, S. 1995a. Carotenoids from further prasinophytes. *Biochem. Syst. Ecol.* 23:747–55.

Egeland, E. S., Guillard, R. R. L. & Liaaen-Jensen, S. 1997. Additional carotenoid prototype representatives and a general chemosystematic evaluation of carotenoids in Prasinophyceae (Chlorophyta). *Phytochemistry* 44:1087–97.

Egeland, E. S., Johnsen, G., Eikrem, W., Throndsen, J. & Liaaen-Jensen, S. 1995b. Pigments of *Bathycoccus prasinos* (Prasinophyceae): methodological and chemosystematic implications. *J. Phycol.* 31:554–61.

Fawley, M. W. 1992. Photosynthetic pigments of *Pseudoscourfieldia marina* and selected green flagellates and coccoid ultraphytoplankton: implications for the systematics of the Micromonadophyceae (Chlorophyta). *J. Phycol.* 28:26–31.

Fawley, M. W. & Lee, C. M. 1990. Pigment composition of the scaly green flagellate *Mesostigma viride* (Micromonadophyceae) is similar to that of the siphonous green alga *Bryopsis plumosa* (Ulvophyceae). *J. Phycol.* 26:666–70.

Fawley, M. W., Qin, M. & Yun, Y. 1999. The relationship between *Pseudoscourfieldia marina* and *Pycnococcus provasolii* (Prasinophyceae, Chlorophyta): evidence from 18S rDNA sequence data. *J. Phycol.* 35:838–43.

Fawley, M. W., Yun, Y. & Qin, M. 2000. Phylogenetic analyses of 18S rDNA sequences reveal a new coccoid lineage of the Prasinophyceae (Chlorophyta). *J. Phycol.* 36:387–93.

Guillard, R. R. L., Keller, M. D., O'Kelly, C. J. & Floyd, G. L. 1991. *Pycnococcus provasolii* gen. et sp. nov; a coccoid prasinoxanthin-containing phytoplankter from the western North Atlantic and Gulf of Mexico. *J. Phycol.* 27:39–47.

Hillis, D. M. & Huelsenbeck, J. P. 1992. Signal, noise, and reliability in molecular phylogenetic analyses. *J. Hered.* 83:189–95.

Hooks, C. E., Bidigare, R. R., Keller, M. D. & Guillard, R. R. L. 1988. Coccoid eukaryotic marine ultraplankters with four different HPLC pigment signatures. *J. Phycol.* 24:571–80.

Jeffrey, S. W. 1989. Chlorophyll *c* pigments and their distribution in the chromophyte algae. *In* Green, J. C. & Leadbeater, B. S. C. [Eds.] *The Chromophyte Algae: Problems and Perspectives.* Clarendon Press, Oxford, pp. 13–36.

Jeffrey, S. W., Mantoura, R. F. C. & Bjørnland, T. 1997. Data for identification of 47 key pigments. *In* Jeffrey, S. W., Mantoura, R. F. C. & Wright, S. W. [Eds.] *Phytoplankton Pigments in Oceanography.* UNESCO, Paris, pp. 343–60.

Jeffrey, S. W. & Vesk, M. 1997. Introduction to marine phytoplankton and their pigment signatures. *In* Jeffrey, S. W., Mantoura, R. F. C. & Wright, S. W. [Eds.] *Phytoplankton Pigments in Oceanography.* UNESCO, Paris, pp. 37–84.

Keller, M. D., Selvin, R. C., Claus, W. & Guillard, R. R. L. 1987. Media for the culture of oceanic ultraphytoplankton. *J. Phycol.* 23:633–8.

Kohata, K. & Watanabe, M. 1989. Diel changes in the composition of photosynthetic pigments and cellular carbon and nitrogen in *Pyramimonas parkeae* (Prasinophyceae). *J. Phycol.* 25:377–85.

Maddison, W. P. & Maddison, D. R. 1992. *MacClade: Analysis of Phylogeny and Character Evolution. V.3.0.* Sinauer, Sunderland, Massachusetts.

Manton, I. 1959. Electron microscopical observations on a very small flagellate: the problem of *Chromulina pusilla. J. Mar. Biol. Assoc. U.K.* 38:319–33.

Manton, I. 1977. *Dolichomastix* (Prasinophyceae) from arctic Canada, Alaska and South Africa: a new genus of flagellates with scaly flagella. *Phycologia* 16:427–38.

Marin, B. & Melkonian, M. 1994. Flagellar hairs in prasinophytes (Chlorophyta): ultrastructure and distribution on the flagellar surface. *J. Phycol.* 30:659–78.

Melkonian, M. 1990. Prasinophyceae. *In* Margulis, L., Corliss, J. O., Melkonian, M. & Chapman, D. J. [Eds.] *Handbook of Protoctista.* Jones and Bartlett Publishers, Boston, pp. 600–7.

Moestrup, Ø. 1984. Further studies on *Nephroselmis* and its allies (Prasinophyceae). II. *Mamiella* gen. nov., Mamiellaceae fam. nov., Mamiellales ord. nov. *Nord. J. Bot.* 4:109–21.

Moestrup, Ø. 1990. Scale structure in *Mantoniella squamata*, with some comments on the phylogeny of the Prasinophyceae (Chlorophyta). *Phycologia* 29:437–42.

Moestrup, Ø. 2000. The flagellate cytoskeleton. *In* Leadbeater, B. S. C. & Green, J. C. [Eds.] *The Flagellates.* Francis & Taylor, London, pp. 69–94.

Moestrup, Ø. & Thomsen, H. A. 1980. Preparation of shadowcast whole mounts. *In* Gantt, E. [Ed.] *Handbook of Phycological Methods. Developmental and Cytological Methods.* University Press, Cambridge, pp. 385–90.

Moestrup, Ø. & Throndsen, J. 1988. Light and electron microscopical studies on *Pseudoscourfieldia marina*, a primitive scaly green flagellate (Prasinophyceae) with posterior flagella. *Can. J. Bot.* 66:1415–34.

Nakayama, T., Kawachi, M. & Inouye, I. 2000. Taxonomy and phylogenetic position of a new prasinophycean alga, *Crustomastix didyma* gen. & sp. nov. (Chlorophyta). *Phycologia* 39:337–48.

Nakayama, T., Marin, B., Kranz, H. D., Surek, B., Huss, V. A. R., Inouye, I. & Melkonian, M. 1998. The basal position of scaly green flagellates among the green algae (Chlorophyta) is revealed by analyses of nuclear-encoded SSU rRNA sequences. *Protist* 149:367–80.

Posada, D. & Crandall, K. A. 1998. Modeltest: testing the model of DNA substitution. *Bioinformatics* 14:817–8.

Rambaud, A. 1995. Se-Al, sequence alignment program v1-d1, Department of Zoology, University of Oxford.

Ricketts, T. R. 1970. The pigments of Prasinophyceae and related organisms. *Phytochemistry* 9:1835–42.

Rowan, R. & Powers, D. A. 1992. Ribosomal RNA sequences and the diversity of symbiotic dinoflagellates (zooxanthellae). *Proc. Natl. Acad. Sci. USA* 89:3639–43.

Schimek, C., Stadnichuck, I. N., Knaust, R. & Wehrmeyer, W. 1994. Detection of chlorophyll c_1 and magnesium-2,4-divinylpheoporphyrin a_5 monomethylester in cryptophytes. *J. Phycol.* 30: 621–7.

Simon, N., Barlow, R. G., Marie, D., Partensky, F. & Vaulot, D. 1994. Characterization of oceanic photosynthetic picoeukaryotes by flow cytometry. *J. Phycol.* 30:922–55.

Steinkötter, J., Bhattacharya, D., Semmelroth, I., Bibeau, C. & Melkonian, M. 1994. Prasinophytes from independent lineages within the Chlorophyta: evidence from ribosomal RNA sequence comparisons. *J. Phycol.* 30:340–5.

Swofford, D. L. 2001. *PAUP* Phylogenetic Analysis Using Parsimony (*and Other Methods)*, version 4.0b8. Sinaer Associates, Sunderland, Massachusetts.

Sym, S. D. & Pienaar, R. N. 1993. The class Prasinophyceae. *Prog. Phycol. Res.* 9:281–376.

Throndsen, J. & Zingone, A. 1997. *Dolichomastix tenuilepis* sp. nov., a first insight in the microanatomy of the genus *Dolichomastix* (Mamiellales, Prasinophyceae, Chlorophyta). *Phycologia* 36: 244–54.

Vidussi, F., Claustre, H., Bustillos-Guzman, J., Caillau, C. & Marty, J.-C. 1996. Determination of chlorophylls and carotenoids of marine phytoplankton: separation of chlorophyll *a* from divinylchlorophyll *a* and zeaxanthin from lutein. *J. Plankton Res.* 18:2377–82.

Wilhelm, C., Kolz, S., Meyer, M., Schmitt, A., Zuber, H., Egeland, E. S. & Liaan-Jensen, S. 1997. Refined carotenoid analysis of the major light-harvesting complex of *Mantoniella squamata. Photosynthetica* 33:161–71.

Wilhelm, C., Lenartz-Weiler, I., Wiedeman, I. & Wild, A. 1986. The light-harvesting system of a *Micromonas* species (Prasinophyceae): the combination of three different chlorophyll species in one sign chlorophyll-protein complex. *Phycologia* 25: 304–12.

Yokohama, Y. 1981. Distribution of the green algae light-absorbing pigments siphonaxanthin and siphonein in marine green algae. *Bot. Mar.* 24:637–40.

Yokohama, Y. 1983. A xanthophyll characteristic of deep-water green algae lacking siphonaxanthin. *Bot. Mar.* 26:45–8.

Zingone, A., Throndsen, J. & Forlani, G. 1995. *Pyramimonas oltmannsii* (Prasinophyceae) reinvestigated. *Phycologia* 34:241–9.